Biogeosciences Discuss., https://doi.org/10.5194/bg-2017-286
Manuscript under review for journal Biogeosciences
Discussion started: 11 July 2017
© Author(s) 2017. CC BY 4.0 License.

Towards an assessment of riverine dissolved organic carbon in surface waters of the Western Arctic Ocean based on remote sensing and biogeochemical modeling

[1]Vincent Le Fouest
[2,3]Atsushi Matsuoka
[4]Manfredi Manizza
[1]Mona Shernetsky
[5]Bruno Tremblay
[2,3]Marcel Babin

[1]Littoral Environnement et Sociétés, UMR 7266, Université de La Rochelle, La Rochelle, France

[2]Takuvik Joint International Laboratory, Université Laval & CNRS, Québec, QC, G1V 0A6, Canada

[3]Takuvik Joint International Laboratory, CNRS, Québec, QC, G1V 0A6, Canada

[4]Geosciences Research Division, Scripps Institution of Oceanography, University of California San Diego, La Jolla, CA 92093-0244, USA

[5]Department of Atmospheric and Oceanic Sciences, McGill University, Montreal, QC, H3A OB9, Canada

Biogeosciences Discuss., https://doi.org/10.5194/bg-2017-286
Manuscript under review for journal Biogeosciences
Discussion started: 11 July 2017
© Author(s) 2017. CC BY 4.0 License.

Abstract

Future climate warming of the Arctic could potentially enhance the load of riverine dissolved organic carbon (RDOC) of Arctic rivers due to increased carbon mobilization within watersheds. A greater flux of RDOC might thus impact the biogeochemical processes of the coastal Arctic Ocean (AO). In this study, we show that estimates of RDOC concentrations in the surface waters of the Canadian Beaufort Sea computed for 2003-2011 by both optical remote sensing and a physical-biogeochemical coupled model compare favorably. Our results suggest that, over spring-summer, RDOC contributes to 35 % of primary production and that an equivalent of ~10 % of the riverine RDOC is exported westwards with a potential for fueling the biological production of the eastern Alaskan nearshore waters. The combination of model and satellite data can be extended to the entire AO to quantify the expected changes in RDOC fluxes and their potential impact on AO biogeochemistry. This is left for future work.

Biogeosciences Discuss., https://doi.org/10.5194/bg-2017-286
Manuscript under review for journal Biogeosciences
Discussion started: 11 July 2017
© Author(s) 2017. CC BY 4.0 License.

1. Introduction

The Arctic Ocean (AO) receives ~10% of the global freshwater discharge (Serreze et al., 2006) of which the larger part (~64%) originates from eight main pan-Arctic rivers (Holmes et al., 2012). Over the past 30 years, the intensification of the Arctic freshwater cycle linked to increasing precipitations (Rawlins et al., 2010) resulted into an increase of the freshwater discharge by ~2.6 % and ~3.1 % per decade from North American and Eurasian rivers, respectively (Holmes et al., 2015). The permafrost of the surrounding watersheds contains more than half the soil carbon stock on Earth (Tarnocai et al., 2009). With the warming of the lower atmosphere, the permafrost undergoes a substantial thawing likely to alter the organic carbon (OC) content and quality of inland waters (Romanovsky et al., 2010). At the Mackenzie River mouth, the riverine dissolved organic carbon (RDOC) flux increased by ~39 % over the past 40 years (Tank et al., 2016).

Coastal waters influenced by river plumes are hence exposed to changing conditions in terms of OC flux from land. After the seasonal ice melt and breakup, a fraction of the OC pool is transported by the seasonal river flow towards the coastal ocean. In river waters, the dissolved OC is present in higher concentration than the particulate form (Le Fouest et al., 2013; Dittmar et al., 2003), accounting for more than 85 % of the total terrigenous OC flux (McGuire et al., 2009). The pan-Arctic flux of RDOC (37.7 TgC yr^{-1}; Manizza et al., 2009; Raymond et al., 2007; Opsahl et al., 1999) is hence a significant pool of the carbon cycle. For comparison, it represents ~10 % to ~19 % of the carbon fixed by phytoplankton in the whole AO (Stein and Macdonald, 2004; Bélanger et al., 2013) and reaches ~34 % of primary production in the oligotrophic Beaufort Sea (Manizza et al., 2009; S. Bélanger, pers. comm.) RDOC can markedly modify the biological production and biogeochemistry of the AO waters. Its degradation is partly responsible for the acidification of the East Siberian shelf waters (Semiletov et al., 2016). Within the pelagic food web, RDOC can be assimilated and transformed, promoting phytoplankton and bacterioplankton production (Le Fouest et al., 2015; Tank et al., 2012). Furthermore, RDOC can modulate the air-sea fluxes of carbon dioxide at the pan-Arctic scale lowering by 10 % the carbon uptake of the AO in present climatic

© Author(s) 2017. CC BY 4.0 License.

conditions (Manizza et al., 2011).

In recent studies, RDOC flux data were used in a 3D ocean-biogeochemical coupled model to investigate the fate of RDOC within surface Arctic waters (Le Fouest et al., 2015; Manizza et al., 2013, 2011, 2009). However, simulated spatial and temporal change in RDOC concentrations have not yet been compared with remote sensing data to assess the model predictive ability. Such a model-satellite comparison allows validating the model and then using it with confidence to resolve the annual cycle of RDOC, a prerequisite for a robust assessment of the RDOC contribution to the Arctic carbon cycle. To this end, sea surface RDOC concentrations were estimated for the Canadian Beaufort Sea using a 3D ocean-biogeochemical coupled model (Le Fouest et al., 2015) and satellite optical remote sensing. Our goals are to compare RDOC data derived from the model and from remote sensing using skill metrics, to assess the model capacity to reproduce the observed seasonal and spatial variability in RDOC, and to provide bulk estimates of the seasonal RDOC stock and lateral fluxes within the surface coastal waters using a combination of these two approaches.

The paper is organized as follows. First, we describe the two different approaches used to quantify RDOC within the AO, i.e. a semi-analytical method based on remote sensing and a regional ocean-biogeochemical coupled model that includes explicit fluxes of RDOC to the AO. Second, we compare the distribution and export flux of RDOC within surface waters of the Beaufort Sea estimated by the model and remote sensing. Finally, we discuss future developments of biogeochemical models necessary to simulate successfully the carbon budget of Arctic coastal waters in a warming world.

2. Material and methods

2.1 Remote sensing data

Monthly composites of remotely sensed RDOC concentrations are calculated from June to September for the 2003-2011 time periods at a 1 km horizontal resolution. RDOC concentrations were estimated from remote sensing data in two separate steps. First, the light absorption

Biogeosciences Discuss., https://doi.org/10.5194/bg-2017-286
Manuscript under review for journal Biogeosciences
Discussion started: 11 July 2017
© Author(s) 2017. CC BY 4.0 License.

89 coefficients of colored dissolved organic matter at 443 nm ($a_{CDOM}(443)$) were derived by applying a
90 semi-analytical algorithm to ocean color data (Matsuoka et al., 2013). Second, an empirical
91 relationship between RDOC concentrations and $a_{CDOM}(443)$ established for the southern Beaufort
92 Sea (Matsuoka et al., 2012) was applied to the satellite-derived $a_{CDOM}(443)$ (Matsuoka et al., 2014,
93 2013). Using ocean color data shows that estimates of RDOC have a mean uncertainty of 28 %
94 (Matsuoka et al., in revision).
95
96 **2.2 3D physical-biogeochemical model data**
97 We used the MITgcm (MIT general circulation model) ocean-sea ice-biogeochemistry coupled
98 model (Lee et al., 2016; Le Fouest et al., 2015) to simulate the RDOC concentrations at the pan-
99 Arctic scale with a special focus on the Beaufort Sea where the remote sensing data were analyzed.
100 The MITgcm ocean-sea ice model (Nguyen et al., 2011, 2009; Losch et al., 2010; Condron et al.,
101 2009) has a variable horizontal resolution of ~18 km and covers the Arctic domain with open
102 boundaries at 55°N on the Atlantic Ocean and Pacific Ocean sides. The open ocean boundaries are
103 constrained by potential temperature, salinity, flow, and sea-surface elevation derived from
104 integrations of a global configuration of the MITgcm model (Menemenlis et al., 2005). Atmospheric
105 forcings (10 m winds, 2 m air temperature and humidity, and downward long and short-wave
106 radiation) are taken from the six-hourly data sets of the Japanese 25 year ReAnalysis (JRA-25)
107 (Onogi et al., 2007). In addition to precipitations, the hydrologic forcing includes a monthly
108 climatology of freshwater discharge from 10 pan-arctic watersheds (Manizza et al., 2009). Monthly
109 mean estuarine fluxes of freshwater are based on an Arctic Runoff database (Lammers et al., 2001;
110 Shiklomanov et al., 2000). The riverine forcing is associated with a monthly climatology of RDOC
111 discharge specific to each watershed (Manizza et al., 2009). The total annual load of RDOC is 37.7
112 TgC yr^{-1}, which is consistent with the estimate of Raymond et al. (2007). The physical model is
113 coupled with a 10-compartment biogeochemical model. A full description of the biogeochemical
114 model is given in Le Fouest et al. (2015). It explicitly accounts for dissolved inorganic nutrients

Biogeosciences Discuss., https://doi.org/10.5194/bg-2017-286
Manuscript under review for journal Biogeosciences
Discussion started: 11 July 2017
© Author(s) 2017. CC BY 4.0 License.

115 (nitrate and ammonium), small and large phytoplankton, protozooplankton, mesozooplankton,
116 bacterioplankton, detrital particulate and dissolved organic nitrogen, and RDOC (Lee et al., 2016;
117 Le Fouest et al., 2015). The RDOC compartment couples the marine and terrestrial cycling of
118 organic matter though RDOC recycling into inorganic nutrients by bacterioplankton. According to
119 Wickland et al. (2012), 15% of the RDOC entering the model is usable by bacterioplankton.
120 Monthly averages of surface RDOC concentrations are obtained from the study of Le Fouest et al.
121 (2015) for June, July, August and September over 2003-2011 at an 18 km horizontal resolution.
122
123 **2.3 Analysis**
124 Remotely sensed and simulated RDOC data were binned for the months of June, July, August and
125 September over the 9-year period to get the best areal coverage in the satellite composites. The
126 remotely sensed RDOC concentrations were regridded on the model horizontal grid. Skill metrics
127 were used to compare the remotely sensed estimates of RDOC (sat) with their simulated
128 counterparts (mod). The metrics included the correlation coefficient (r), the unbiased root mean
129 square error (RMSE), the Nash-Sutcliffe model efficiency index (MEF), the geometric bias, and the
130 geometric RMSE (Stow et al., 2009; Doney et al., 2009; Nash and Sutcliffe, 1970). The metrics are
131 computed as follows:
132

$$r = \frac{\sum_{n=1}^{N}(sat_n - \overline{sat})\left(mod_n - \overline{mod}\right)}{\sqrt{\sum_{n=1}^{N}(sat_n - \overline{sat})^2 \sum_{n=1}^{N} mod_n - \overline{mod^2}}} \qquad (Eq.1)$$

$$unbiased\ RMSE = \sqrt{\frac{1}{N}\sum_{n=1}^{N}\left(mod_n - sat_n - \left(\overline{mod} - \overline{sat}\right)\right)^2} \qquad (Eq.2)$$

$$MEF = \frac{\sum_{n=1}^{N}(sat_n - \overline{sat})^2 - \sum_{n=1}^{N}(sat_n - mod_n)^2}{\sum_{n=1}^{N}(sat_n - \overline{sat})^2} \qquad (Eq.3)$$

$$geometric\ bias = e^{(\overline{mod} - \overline{sat})} \qquad (Eq.4)$$

Biogeosciences Discuss., https://doi.org/10.5194/bg-2017-286
Manuscript under review for journal Biogeosciences
Discussion started: 11 July 2017
© Author(s) 2017. CC BY 4.0 License.

$$geometric\ RMSE = \sqrt{e^{\left(\frac{1}{N}\sum_{n=1}^{N}(mod_n - sat_n)^2\right)}} \qquad (Eq.5)$$

where N is the number of RDOC data, and $\overline{sat}$ and $\overline{mod}$ are the remotely sensed and the simulated RDOC averages, respectively. Monthly fluxes of RDOC were computed along two cross-shelf transects (see upper-middle panel in Fig. 1) as the product of the sea surface currents velocities simulated by the model with the remotely sensed or simulated RDOC concentrations.

3. Results and discussion

3.1 RDOC concentrations and distribution

Over the Mackenzie shelf, the plume of high-RDOC (> 120 mmolC m^{-3}) had a maximal areal extent in June for both the model and the satellite data (Fig. 1). This coincided with the seasonal peak of river discharge in June as parameterized in the model and generally depicted by in-situ time series (Yang et al., 2015). From July to September, the high-RDOC areal extent progressively decreased following the seasonal pattern of riverine freshwater discharge (see Yang et al., 2015; Manizza et al., 2009). This seasonal pattern was observed both in the model and satellite data. The simulated RDOC concentrations were lower than in the satellite record in Mackenzie Bay and east of the Mackenzie Bay, especially in June (by 44 % in average) and July (by 27 % in average). Terrigenous DOC originating from both melted sea ice and permafrost erosion along the coastline were not taken into account in the model. First year sea ice represents a carbon flux of 2 10^{-4} TgC yr^{-1} within the Chukchi and Beaufort seas (Rachold et al., 2004). This flux is 4 orders of magnitude lower than the RDOC flux from the Mackenzie River specified as boundary conditions in the model (2.54 TgC yr^{-1}). Similarly, DOC eroded from permafrost stored in the Canadian Arctic shores accounts for only ~ 0.5 10^{-4} (Tanski et al., 2016) to ~ 1.6 10^{-4} TgC yr^{-1} (Ping et al., 2011, using a DOC:POC ratio of 1:900 as in Tanski et al., 2016). These two sources of terrigenous DOC, not parameterized in the model, are not believed to explain the model-satellite discrepancies in RDOC (Fig. 1). Other factors

© Author(s) 2017. CC BY 4.0 License.

157 might contribute to these model-satellite differences observed nearshore. First, the model does not
158 distinguish between the two main pathways of the Mackenzie River discharge entering the shallow
159 delta zone. In June, the Mackenzie Bay receives most of the fresh and turbid river water (~66 %)
160 while the remaining ~33 % spreads east of the delta in Kugmallit Bay (Davies, 1975). This pattern
161 was particularly well captured by the remotely sensed data in June-July (Fig. 1). Second, the inner
162 Mackenzie shelf (< 20 m) is bounded during winter by a thick ridged ice barrier grounded on the
163 sea floor called stamukhi (Macdonald et al., 1995). The stamukhi retains the turbid river water
164 within the inner shelf in winter. When sea ice breaks up and the freshet reaches its seasonal
165 maximum in June, the retained turbid waters spread farther within the coastal zone. The remote
166 sensing data could resolve this particular feature in June (see Fig. 1) explaining the higher RDOC
167 concentrations observed nearshore. Such a pattern is also reported for terrigenous particulate
168 organic matter (Doxaran et al., 2015). Farther on the Mackenzie shelf, as delimited by the 300 m
169 isobaths remotely sensed and simulated concentrations of RDOC were both within the range of
170 values measured in spring (~110-230 mmolC m^{-3}; Osburn et al., 2009) and summer (~60-100
171 mmolC m^{-3}; Para et al., 2014). Overall, the model and the satellite data captured the seasonal cycle
172 and spatial distribution of RDOC concentrations in the study area.

173 Skill metrics were computed over the whole study area (see Fig. 1) to provide a quantitative
174 comparison of RDOC simulated with the model and satellite data (Table 1). For all months, the
175 correlation coefficient was relatively high ($0.78<r<0.82$) within the range of values obtained for sea
176 surface dissolved inorganic nutrients simulated by global models ($r>0.75$; see Doney et al., 2009).
177 Regardless of amplitude, the r values showed that the simulated and remotely sensed RDOC
178 concentrations presented similar patterns of variation. The size of the model-satellite discrepancies
179 was given by the unbiased RMSE. Overall, the unbiased RMSE decreased from June (41.4 mmolC
180 m^{-3}) to September (29.3 mmolC m^{-3}). This result suggested that the model was more accurate after
181 the seasonal peak of river discharge occurring in June in agreement with Manizza et al. (2009) and
182 Yang et al. (2015). The model capability for predicting RDOC relative to the average of the remote

Biogeosciences Discuss., https://doi.org/10.5194/bg-2017-286
Manuscript under review for journal Biogeosciences
Discussion started: 11 July 2017
© Author(s) 2017. CC BY 4.0 License.

sensing counterparts was estimated by the model efficiency index (1≥MEF>-∞) (Nash and Sutcliffe, 1970). The higher the MEF, the closer is the match between the model and the observations. The metric was positive for all months suggesting that the satellite-derived RDOC average was not a better predictor than the simulated RDOC data. The MEF reached the highest values in June-July (0.49-0.6), i.e. during and just after the seasonal peak of river discharge. This suggested that despite a relatively higher dispersion measured in June-July by the unbiased RMSE the model could reliably predict the RDOC concentrations remotely sensed during the seasonal peak of discharge. Metrics based on log-transformed RDOC data were also computed to give more even weight to all of the data and not skew the statistics towards the largest values. For all months, the geometric bias (1.03-1.1) was higher than one meaning that the model tended, on average, to overestimate the observations over the whole domain. The higher geometric bias was reported in August (1.13), when the river discharge was low, suggesting that RDOC removal was likely underestimated in the model in late summer. The geometric RMSE was close to one for all months suggesting that the typical error at any point of domain was much lower in magnitude than the observed RDOC value. A Taylor diagram (Taylor, 2001) was produced to provide a synthetic and complementary overview of how the simulated and remotely sensed RDOC concentrations compared seasonally in terms of correlation, amplitude of variations (given by the standard deviations), and normalized model-satellite discrepancies (Fig. 2). All months differed by their normalized RMSE and amplitude of variations while the correlation coefficient was close to ~0.8 (see Table 1). The model best performed in simulating RDOC in July, just after the seasonal peak of river discharge, followed by the months of June and August. June and August were very close despite distinct seasonal patterns of river discharge (high and low, respectively), whereas September showed the highest model-satellite data dispersion. With respect to satellite estimates, the skill metrics overall suggested that the model could reliably simulate RDOC concentrations in surface waters over a wide range of river discharge and RDOC load.

Biogeosciences Discuss., https://doi.org/10.5194/bg-2017-286
Manuscript under review for journal Biogeosciences
Discussion started: 11 July 2017
© Author(s) 2017. CC BY 4.0 License.

3.2 RDOC stock and lateral export fluxes

The overall agreement between the model and the satellite RDOC concentration allowed the assessment of the mean areal stock and lateral fluxes of RDOC using the mean surface ocean circulation simulated by the MITgcm (Table 2). The monthly mean RDOC areal stock (June to September) over the Mackenzie shelf as delimited by the 300 m isobaths was estimated to 1.37 TgC (Table 2). The bias between the model and the satellite data was the highest in August but did not exceed +8.2 % (0.1 Tg C). This result is consistent with the highest geometric bias reported in August (Table 1). In the model, the removal of RDOC through photo-oxidation (Bélanger et al., 2006) was not taken into account. Assuming annual mean mineralization rate of RDOC of ~0.02 Tg C (Bélanger et al., 2006), this process would explain <2 % of the reported RDOC difference. In the model, bacterioplankton consumed RDOC to produce ammonium usable in turn by phytoplankton. In the Beaufort Sea, this pathway contributed to primary production by 35 % on average over 2003-2011. However, the simulated rates of bacterioplankton production (<30 mgC m^{-2} d^{-1}) still remained in the lower range of those measured in the Beaufort Sea (25-68 mgC m^{-2} d^{-1}; Ortega-Retertua et al., 2012; Vallières et al., 2008). The likely underestimation of the RDOC removal by bacterioplankton in the model during summer months might also contribute to the reported bias between the model and the satellite data. Nevertheless, the bias remained moderate with respect to values reported for June, July and September (-1.5 % to -2.8 %) (Table 2).

Combining the modeling and remote sensing approaches allowed for the reconstruction of the dominant surface pattern in lateral RDOC fluxes in the Canadian Beaufort Sea from June to September (Fig. 3). Two north-south transects were defined east (Cape Bathurst) and west (Mackenzie Trough) of the Mackenzie shelf (see upper-middle panel in Fig. 1). The net seasonal flux was westward along the two transects following the anticyclonic circulation pattern of the Beaufort gyre (Mulligan et al., 2010) and was maximum in June and September. The flux was at least three times higher along the western transect near the Mackenzie Through than east at Cape Bathurst. This suggests a net export of RDOC towards the Alaskan part of the Beaufort Sea. In

© Author(s) 2017. CC BY 4.0 License.

contrast, whilst the flux in July and August remained oriented westward near the Mackenzie Trough, it was reversed at Cape Bathurst. In July, the RDOC flux was still 1.3 to 1.7 times higher along the western transect. In August, however, there was more RDOC (~1.4-fold) exported eastward at Cape Bathurst than exported westward near the Mackenzie Through.

Along the two transects, the simulated fluxes were higher than those derived from remotely sensed RDOC concentrations (Fig. 3). The monthly bias between the model and the satellite flux estimates varied between 0 % and +18.2 %. The bias on the seasonal net flux was moderate (+8.3 %) near the Mackenzie Trough but reached +25 % at Cape Bathurst. The seasonal mean flux however was one order of magnitude lower than near the Mackenzie Trough. The flux estimates suggested that, despite discrepancies in RDOC concentrations, the modeling and remote sensing approaches provided robust estimates of the lateral transport of RDOC in surface waters in late spring-summer. Because of sea ice and cloud cover, the satellite retrieval was limited to a temporal window covering a third of a year only, i.e. from June to September. The yearly mean lateral flux of RDOC was computed from the simulated data along the Mackenzie Trough transect and it reached 0.31 TgC. The flux of RDOC cumulated over June to September along this transect (0.12-0.13 TgC) represented ~42 % of this annual flux (0.31 TgC), which is consistent with the fraction of the annual discharge of freshwater by the Mackenzie that occurs during spring-summer (~50 %; McClelland et al., 2012). Using stable isotope techniques on pelagic particulate organic matter, Bell et al. (2016) showed that OC originating from the Mackenzie outflow in summer was incorporated within bentho-pelagic food webs as far as the eastern Alaskan shelf. In nearshore waters of this part of the Beaufort Sea, the study of Dunton et al. (2006) using stable isotopes also suggested that RDOC from the Mackenzie River could add to the local terrigenous carbon inputs mediated by coastal erosion and smaller rivers to fuel the biological production in summer. Using the model and satellite data, we report that an equivalent of ~10 % (0.12-0.13 TgC) of the cumulated flux of RDOC delivered by the Mackenzie River over spring-summer (1.32 TgC) was exported westward in the Alaskan Beaufort Sea along the Mackenzie Trough transect.

© Author(s) 2017. CC BY 4.0 License.

261

262 **4. Perspectives**

263 The results of our study suggest that the model is in fair agreement with the surface RDOC fields
264 remotely sensed in spring-summer. The comparison allows an evaluation of the model and justifies
265 its use to resolve the annual cycle of RDOC. Because remote sensing data provide data only during
266 spring-summer, further uncertainties still remain in the model in fall-winter. In addition, the model
267 involves some limitations mostly due to the biogeochemical processing of RDOC, which is
268 complex to translate into robust mechanistic equations as highly dependent on the availability of in-
269 situ data in Arctic waters. In the model, the RDOC compartment is split into a labile and a non-
270 labile fraction (see Le Fouest et al., 2015). This parameterization strongly constrains the removal of
271 RDOC by bacterioplankton and therefore its concentrations simulated in surface waters. In natural
272 waters, however, RDOC is made of a complex mixture of compounds that differ by their chemical
273 composition and age (Mann et al., 2016) and so along the seasons (Wickland et al., 2012).
274 Therefore, a more realistic representation in the model of the nature of the organic matter entering
275 the coastal waters, including the riverine flux of dissolved organic nitrogen, along with an improved
276 C:N stoichiometry of bacterioplankton uptake (Le Fouest et al., 2015) might improve the simulated
277 RDOC concentrations.
278 Furthermore, the quantification of the RDOC flux from the watersheds to the coastal AO is another
279 key issue to addressing its role in the biogeochemistry of shelf waters. Recently, watersheds models
280 were developed to assess this flux (Tank et al., 2016; Kicklighter et al., 2013; Holmes et al., 2012).
281 Such models provide realistic estimates but still require improvements as watersheds properties and
282 mechanistic processes underlying the RDOC mobilization and riverine transport are complex to set
283 up (see Kicklighter et al., 2013). In a recent study, the remote sensing of high resolution ocean color
284 data was used to assess RDOC concentrations during the open water season along a large Eurasian
285 river (Herrault et al., 2016). Ocean color techniques could then prove useful in the future to improve
286 the RDOC time series set at model boundaries by accounting for instance for year-to-year variations

© Author(s) 2017. CC BY 4.0 License.

of RDOC concentrations during the freshet period.

In our study, the RDOC concentrations remotely sensed in shelf waters provide the advantage of already integrating the effect of the watersheds processes such as mobilization, transformation and transport at the seasonal (spring-summer) and synoptic time scales. Therefore, and in regard to the model-satellite data comparison, the assimilation of remotely sensed RDOC data into Arctic models would offer an interesting perspective in the sense it might result in more realistic fields of RDOC simulated in surface waters in spring-summer during high river freshet. Physical and biological data have already been assimilated into Arctic predictive models to make the simulated sea surface temperature, salinity, sea ice extent and thickness, and chlorophyll more reliable (Simon et al., 2015; Massonnet et al., 2015). We may hence expect the assimilation of remotely sensed RDOC concentrations to mitigate, at least partly, the issues linked to setting up realistic RDOC forcings within predictive models. For instance, the assimilation of remotely sensed RDOC data in open waters might help accounting for the interannual variations of RDOC delivered by rivers, which are not resolved by the coupled model that is constrained by a monthly climatology of RDOC load (see Manizza et al., 2009).

Finally, realistic fields of RDOC simulated by Arctic ocean-biogeochemical coupled models would help for a more accurate assessment of CO_2 fluxes at the ocean-atmosphere interface. Arctic models that would combine realistic terrestrial fluxes of organic matter along with a robust representation of the pathways and processes responsible for its transformation in the AO would open an interesting perspective to address the effect on the Arctic carbon cycle of ongoing and future changes in the land-ocean continuum. The increase in seawater temperature of the AO due to global warming (Timmermans, 2016) might promote in the future the metabolism and respiration rates of marine bacterioplankton (Vaquer-Sunyer et al., 2010; Kritzberg et al., 2010). This enhanced microbial activity could then liberate extra nutrients provided by the remineralization of terrigenous organic matter that will then be available for primary production. This process might have an impact not only on the seasonal cycle of PP in the AO but also implications for the higher levels of

© Author(s) 2017. CC BY 4.0 License.

313 the marine food webs of the AO, both benthic and pelagic.

314

315 **Data availability**

316 Data used in this study are available at http://www.obs-lienss.cnrs.fr/Publications/Vincent_LeFouest

317 _data_nc.tar.

318

319 **Acknowledgments**

320 This research was funded by the Centre national d'études spatiales (CNES) grant #131425-BC T23

321 to VLF and the Japan Aerospace Exploration Agency (JAXA) GCOM-C project through grant

322 #16RSTK-007867 to AM. We also thank a joint contribution to the research programs of UMI

323 Takuvik (CNRS & Université Laval), ArcticNet (Network Centres of Excellence of Canada) and the

324 Canada Excellence Research Chair in Remote Sensing of Canada's New Arctic Frontier (MB).

325

Biogeosciences Discuss., https://doi.org/10.5194/bg-2017-286
Manuscript under review for journal Biogeosciences
Discussion started: 11 July 2017
© Author(s) 2017. CC BY 4.0 License.

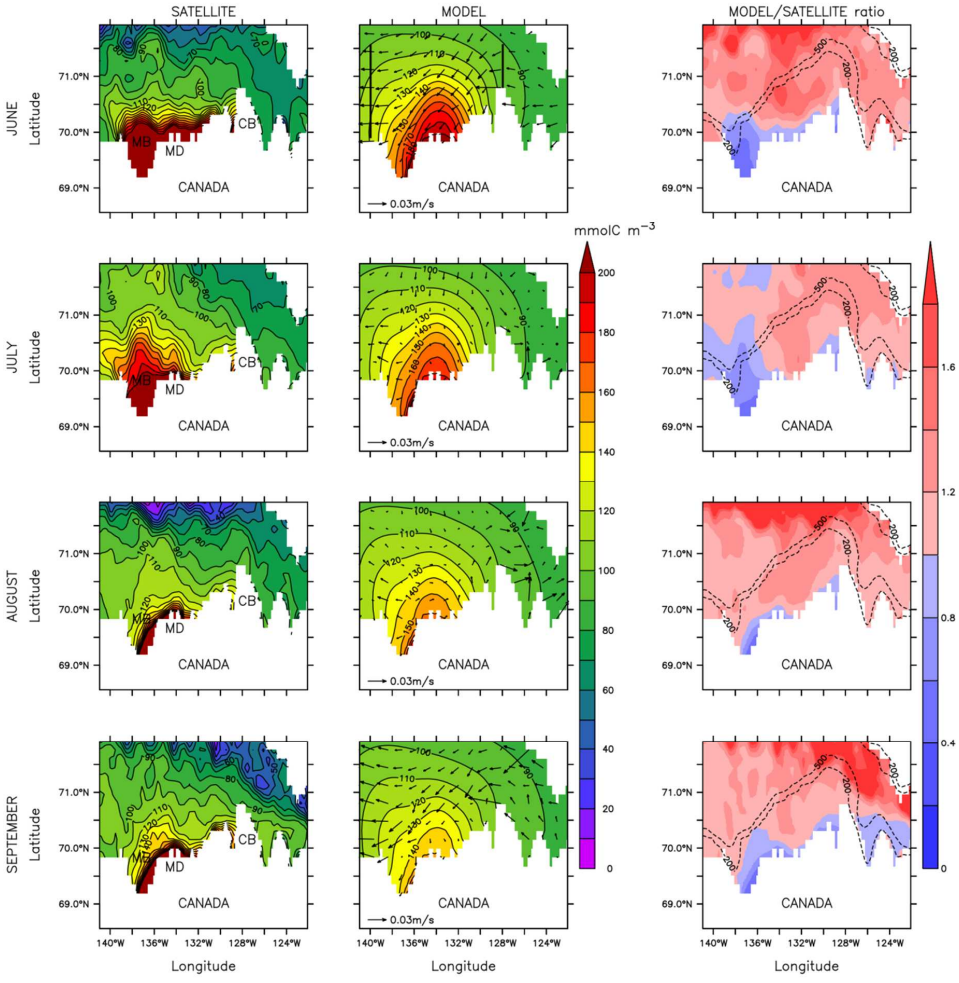

Figure 1. Monthly climatology (2003-2011) of surface RDOC concentration (mmolC m^{-3}) in the Beaufort Sea estimated from remotely sensed ocean color data (left panels) and by the biogeochemical model (middle panels) for June, July, August and September. The Mackenzie Bay (MB), Mackenzie delta (MD) and Cape Bathurst (CB) cited in the text are shown on the left panels. The isolines of RDOC concentration are overlaid (black full lines). In the middle panels, simulated surface currents are overlaid. The two straight lines in the upper-middle panel refer to transects along which surface RDOC fluxes were computed. The right panels show the model over satellite data ratio with the 200 m and 500 m isobaths overlaid.

Biogeosciences Discuss., https://doi.org/10.5194/bg-2017-286
Manuscript under review for journal Biogeosciences
Discussion started: 11 July 2017
© Author(s) 2017. CC BY 4.0 License.

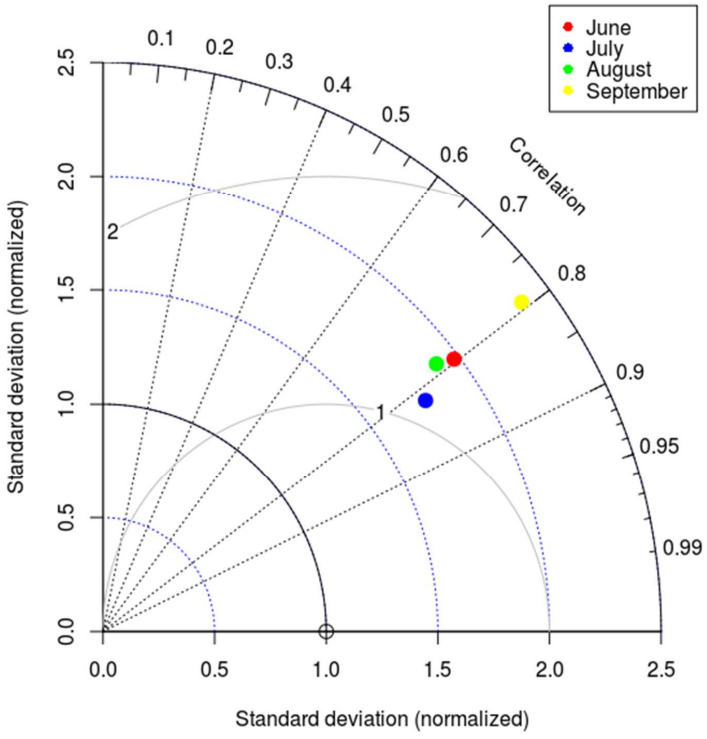

335

336 **Figure 2.** Comparison of simulated and remotely sensed RDOC concentrations using a Taylor
337 diagram. The x-axis and y-axis show the model standard deviation relative to the satellite standard
338 deviation. The open circle on the x-axis represents the reference point. The model-satellite
339 correlation is represented in polar coordinates (angle from the x-axis). The light grey full lines
340 indicate the RMSE relative to the satellite standard deviation.

341

Biogeosciences Discuss., https://doi.org/10.5194/bg-2017-286
Manuscript under review for journal Biogeosciences
Discussion started: 11 July 2017
© Author(s) 2017. CC BY 4.0 License.

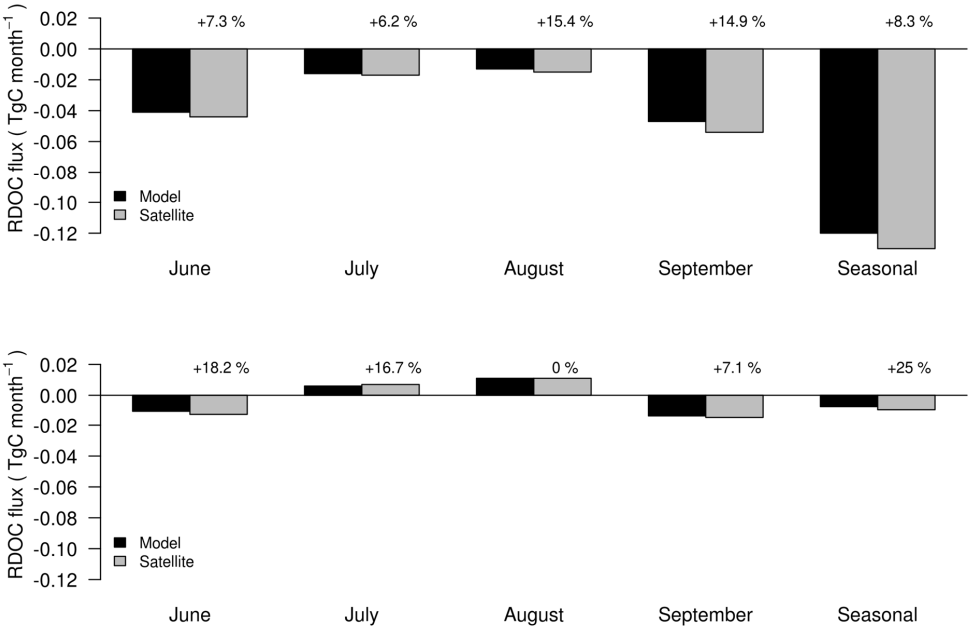

342

343 **Figure 3.** Monthly flux of surface RDOC (TgC month^{-1}) computed along transects located west of
344 the Mackenzie Trough (139°W ; 69.5°N-71°N) (upper panel) and at Cape Bathurst (128°W ;
345 69.5°N-71°N) (lower panel). Transects are shown in figure 1 in the upper-middle panel. Negative
346 values indicate a westward flux. Percentages refer to the model data relative to the satellite data.
347 The seasonal flux refers to the 4-month net flux.

348

Biogeosciences Discuss., https://doi.org/10.5194/bg-2017-286
Manuscript under review for journal Biogeosciences
Discussion started: 11 July 2017
© Author(s) 2017. CC BY 4.0 License.

349 **Table 1.** Skill metrics of comparison computed based on the 2003-2011 monthly climatologies of

350 RDOC.

351

Metric	June	July	August	September
Correlation coefficient	0.79	0.82	0.78	0.79
Unbiased RMSE (mmolC m^{-3})	41.4	29.4	26.0	29.3
Model efficiency	0.49	0.60	0.26	0.38
Geometric statistics using log-transformed data				
Model bias	1.10	1.03	1.13	1.09
RMSE	1.01	1.00	1.02	1.01

352

353

Biogeosciences Discuss., https://doi.org/10.5194/bg-2017-286
Manuscript under review for journal Biogeosciences
Discussion started: 11 July 2017
© Author(s) 2017. CC BY 4.0 License.

354 **Table 2.** Areal stock (TgC) of surface RDOC computed over the Mackenzie shelf (delimited by the
355 300 m isobaths) from the model and satellite data. The bias (%) refers to the model data relative to
356 the satellite data. The seasonal areal stock refers to the 4-month average ± standard deviation.

	June	July	August	September	Seasonal
Model	1.48	1.40	1.32	1.28	1.37±0.07
Satellite	1.51	1.44	1.22	1.30	1.37±0.11
Bias	-2	-2.8	+8.2	-1.5	0

357

358

© Author(s) 2017. CC BY 4.0 License.

References

Bélanger, S., Xie, H., Krotkov, N., Larouche, P., Vincent, W. F., and Babin, M.: Photomineralization of terrigenous dissolved organic matter in Arctic coastal waters from 1979 to 2003: Interannual variability and implications of climate change, Global Biogeochem. Cycles, 20, GB4005, doi:10.1029/2006GB002708, 2006.

Bélanger S., Babin, M., and Tremblay, J.-E.: Increasing cloudiness in Arctic damps the increase in phytoplankton primary production due to sea ice receding, Biogeosciences, 10, 4087–4101, doi:10.5194/bg-10-4087-2013, 2013.

Bell, L. E., Bluhm, B. A., and Iken, K.: Influence of terrestrial organic matter in marine food webs of the Beaufort Sea shelf and slope, Mar. Ecolo. Prog. Ser., 550, 1–24, doi:10.3354/meps11725, 2016.

Condron, A., Winsor, P., Hill, C. N., and Menemenlis, D.: Response of Arctic freshwater budget to extreme NAO forcing, J. Clim., 22, 2422–2437, 2009.

Davies, K. F.: Mackenzie River input to the Beaufort Sea, Beaufort Sea Project, Technical Report 15, Institute of Ocean Sciences, Sidney, British, Columbia, 72 p, 1975.

Dittmar, T., and Kattner, G.: The biogeochemistry of the river and shelf ecosystem of the Arctic Ocean: a review, Mar. Chem., 83, 103–120, doi:10.1016/S0304-4203(03)00105-1, 2003.

Doney, S.C., Lima, I., Moore, J. K., and Takahashi, T.: Skill metrics for confronting global upper ocean ecosytem-biogeochemistry models against field and remote sensing data, J. Mar. Syst., 76, 95–112, doi:10.1016/j.jmarsys.2008.05.015, 2009.

Doxaran, D., Devred, E., and Babin, M.: A 50 % increase in the mass of terrestrial particles delivered by the Mackenzie River into the Beaufort Sea (Canadian Arctic Ocean) over the last 10 years, Biogeosci., 12, 3551–3565, doi:10.5194/bg-12-3551-2015, 2015.

Dunton, K. H., Weingartner, T., and Carmack, E. C.: The nearshore western Beaufort Sea ecosystem: circulation and importance of terrestrial carbon in arctic coastal food webs, Progr. Oceanogr.,

© Author(s) 2017. CC BY 4.0 License.

71, 362–378, doi:10.1016/j.pocean.2006.09.011, 2006.

Herrault, P.-A., Gandois, L., Gascoin, S., Tananaev, N., Le Dantec, T., and Teisserenc, R.: Using high spatio-temporal optical remote sensing to monitor dissolved organic carbon in the Arctic river Yenisei, Remote Sens., 8, 803, doi:10.3390/rs8100803, 2016.

Holmes, R. M., McClelland, J. W., Peterson, B. J., Tank, S. E., Bulygina, E., Eglinton, T. I., Gordeev, V. V., Gurtovaya, T. Y., Raymond, P. A., Repeta, D. J., Staples, R., Striegl, R. G., Zhulidov, A. V., and Zimov, S. A.: Seasonal and annual fluxes of nutrients and organic matter from large rivers to the Arctic Ocean and surrounding seas, Estuar. Coasts, 35, 369–382, doi:10.1007/s12237-011-9386-6, 2012.

Holmes, R. M., Shiklomanov, A. I., Tank, S. E., McClelland, J. W., and Tretiakov, M.: River discharge, Arctic Report Card: Update for 2015, http://www.arctic.noaa.gov/Report-Card/Report-Card-2015/ArtMID/5037/ArticleID/227/River-Discharge, 2015.

Kicklighter, D. W., Hayes, D. J., MacClelland, J. W., Peterson, B. J., McGuire, A. D., and Melillo, J. M.: Insights and issues with simulating terrestrial DOC loading of Arctic river networks, Ecol. App., 23, 1817–1836, doi:10.1890/11-1050.1, 2013.

Kritzberg, E., Duarte, C. M., and Wassmann, P.: Changes in Arctic marine bacterial carbon metabolism in response to increasing temperature, Polar Biol., 33, 1673–1682, doi:10.1007/s00300-010-0799-7, 2010.

Lammers, R. B., Shiklomanov, A. I., Vörösmarty, C. J., Fekete, B. M., and Peterson, B. J.: Assessment of contemporary Arctic river runoff based on observational discharge records, J. Geophys. Res., 106(D4), 3321–3334, doi:10.1029/2000JD900444, 2001.

Lee, Y. J., Matrai, P. A., Friedrichs, M. A. M., Saba, V. S., Aumont, O., Babin, M., Buitenhuis, E. T., Chevallier, M., de Mora, L., Dessert, M., Dunne, J. P., Ellingsen, I., Feldman, D., Frouin, R., Gehlen, M., Gorgues, T., Ilyina, T., Jin, M., John, J. G., Lawrence, J., Manizza, M., Menkes, C. E., Perruche, C., Le Fouest, V., Popova, E., Romanou, A., Samuelsen, A., Schwinger, J.,

© Author(s) 2017. CC BY 4.0 License.

409 Séférian, R., Stock, C. A., Tjiputra, J., Tremblay, B. L., Ueyoshi, K., Vichi, M., Yool, A., and
410 Zhang, J.: Net primary productivity estimates and environmental variables in the Arctic Ocean:
411 An assessment of coupled physical-biogeochemical models, J. Geophys. Res.,
412 doi:10.1002/2016JC011993, 2016.

413 Le Fouest V., Babin, M., and Tremblay, J.-E.: The fate of riverine nutrients on Arctic shelves,
414 Biogeosciences, 10, 3661–3677, doi:10.5194/bg-10-3661-2013, 2013.

415 Le Fouest, V., Manizza, M., Tremblay, B., and Babin, M.: Modeling the impact of riverine DON
416 removal by marine bacterioplankton on primary production in the Arctic Ocean,
417 Biogeosciences, 12, 3385–3402, doi:10.5194/bg-12-3385-2015, 2015.

418 Losch, M., Menemenlis, D., Campin, J.-M., Heimbach, P., and Hill, C.: On the formulation of sea-
419 ice models. Part 1: Effects of different solver implementations and parameterizations, Ocean
420 Model., 33, 129–144, doi:10.1016/j.ocemod.2009.12.008, 2010.

421 McGuire A. D., Anderson, L. G., Christensen, T. R., Dallimore, S., Guo, L., Hayes, D. J., Heimann,
422 M., Lorenson, T. D., Macdonald, R.W., and Roulet, N.: Sensitivity of the carbon cycle in the
423 Arctic to climate change, Ecol. Monogr., 79, 523–555, doi:10.1890/08-2025.1, 2009.

424 Macdonald, R. W., Paton, D. W., Carmack, E. C., and Omstedt, A.: The freshwater budget and
425 under-ice spreading of Mackenzie River water in the Canadian Beaufort Sea based on salinity
426 and 18 O / 16 O measurements in water and ice, J. Geophys. Res., 100, 895–919, 1995, 1995.

427 Manizza, M., Follows, M. J., Dutkiewicz, S., McClelland, J. W., Menemenlis, D., Hill, C. N.,
428 Townsend-Small, A., and Peterson, B. J.: Modeling transport and fate of riverine dissolved
429 organic carbon in the Arctic Ocean, Global Biogeochem. Cycles, 23, GB4006,
430 doi:10.1029/2008GB003396, 2009.

431 Manizza, M., Follows, M., Dutkiewicz, S., Menemenlis, D., McClelland, J. W., Hill, C. N., Peterson,
432 B. J., and Key, R. M.: A model of the Arctic Ocean carbon cycle, J. Geophys. Res., 116(C12),
433 C12020, doi:10.1029/2011JC006998, 2011.

© Author(s) 2017. CC BY 4.0 License.

434 Manizza, M., Follows, M. J., Dutkiewicz, S., Menemenlis, D., Hill, C. N., and Key, R. M.: Changes
435 in the Arctic Ocean CO_2 sink (1996–2007): A regional model analysis, Global Biogeochem.
436 Cycles, 27, 1108–1118, doi:10.1002/2012GB004491, 2013.

437 Mann, P. J., Spencer, R. G. M., Hernes, P. J., Six, J., Aiken, G. R., Tank, S. E., McClelland, J. W.,
438 Butler, K .D., Dyda, R. Y., and Holmes, R. M.: Pan-Arctic Trends in Terrestrial Dissolved
439 Organic Matter from Optical Measurements, Front. Earth Sci., 4, 25, 10.3389/feart.2016.00025,
440 2016.

441 Massonnet, F., Fichefet, T., and Goosse, H.: Prospects for improved seasonal Arctic sea ice
442 predictions from multivariate data assimilation, Ocean Model., 88, 16–25,
443 doi:10.1016/j.ocemod.2014.12.013, 2015.

444 Matsuoka, A., Bricaud, A., Benner, R., Para, J., Sempéré, R., Prieur, L., Bélanger, S., and Babin, M.:
445 Tracing the transport of colored dossolved organic matter in water masses of the Southern
446 Beaufort Sea: relationship with hydrographic characteristics, Biogeosciences, 9, 925–940,
447 doi :10.5194/bg-9-925-2012, 2012.

448 Matsuoka, A., Hooker, S. B., Bricaud, A., Gentili, B., and Babin, M.: Estimating absorption
449 coefficients of colored dissolved organic matter (CDOM) using a semi-analytical algorithm for
450 southern Beaufort Sea waters : application to deriving concentrations of dissolved organic
451 carbon from space, Biogeosci., 10, 917–927, doi :10.5194/bg-10-917-2013, 2013.

452 Matsuoka, A., Babin, M., Doxaran, D., Hooker, S. B., Mitchell, B. G., Bélanger, S., and Bricaud, A.:
453 A synthesis of light absorption properties of the Pan-Arctic Ocean: application to semi-
454 analytical estimates of dissolved organic carbon concentrations from space, Biogeosci., 11,
455 3131–3147, doi:10.5194/bg-11-3131-2014, 2014.

456 Matsuoka, A., Boss, E., Babin, M., Karp-Boss, L., Hafez, M., Chekalyuk, A., Proctor, C. W.,
457 Werdell, P. J., and Bricaud, A.: Pan-Arctic optical characteristics of colored dissolved organic
458 matter: tracing dissolved organic carbon in changing Arctic waters using satellite ocean color

© Author(s) 2017. CC BY 4.0 License.

data, in revision.

McClelland, J. W., Holmes, R. M., Dunton, K. H., and Macdonald, R. W.: The Arctic Ocean estuary, Estuar. Coast., 35, 353–368,doi:10.1007/s12237-010-9357-3, 2012.

Menemenlis, D., Hill, C., Adcroft, A., Campin, J.-M., Cheng, B., Ciotti, B., Fukumori, I., Heimbach, P., Henze, C., Kohl, A., Lee, T., Stammer, D., Taft, J., and Zhang, J.: NASA supercomputer improves prospects for ocean climate research, Eos Trans. AGU, 86, 89–96, 2005.

Mulligan, R. P., Perrie, W., and Solomon, S.: Dynamics of the Mackenzie River plume on the inner Beaufort shelf during an open water period in summer, Estuar. Coast Shelf Sci., 89, 214–220, doi:10.1016/j.ecss.2010.06.010, 2010.

Nash, J., and Sutcliffe, J.: River flow forecasting through conceptual models, part 1 – a discussion of principles, J. Hydrol., 10, 282–290, 1970.

Nguyen, A. T., Menemenlis, D., and Kwok, R.: Improved modeling of the Arctic halocline with a subgrid-scale brine rejection parameterization, J. Geophys. Res., 114, C11014, doi:10.1029/2008JC005121, 2009.

Nguyen, A. T., Menemenlis, D., and Kwok, R.: Arctic ice-ocean simulation with optimized model parameters: Approach and assessment, J. Geophys. Res., 116(C4), C04025, doi:10.1029/2010JC006573, 2011.

Onogi, K., Tsutsui, J., Koide, H., Sakamoto, M., Kobayashi, S., Hatsushika, H., Matsumoto, T., Yamazaki, N., Kamahori, H., Takahashi, K., Kadokura, S., Wada, K., Kato, K., Oyama, R., Ose, T., Mannoji, N., and Taira, R.: The JRA-25 Reanalysis, J. Meteor. Soc. Japan, 85, 369–432, doi:10.2151/jmsj.85.369, 2007.

Opsahl, S., Benner, R., and Amon, R. M.: Major flux of terrigenous dissolved organic matter through the Arctic Ocean, Limnol. Oceanogr., 44, 2017–2023, doi:10.4319/lo.1999.44.8.2017, 1999.

© Author(s) 2017. CC BY 4.0 License.

483 Ortega-Retuerta, E., Jeffrey, W. F., Babin, M., Bélanger, S., Benner, R., Marie, D., Matsuoka, A.,
484 Raimbault, P., and Joux, F.: Carbon fluxes in the Canadian Arctic: patterns and drivers of
485 bacterial abundance, production and respiration on the Beaufort Sea margin, Biogeosciences, 9,
486 3679–3692, doi:10.5194/bg-9-3679-2012, 2012.

487 Raymond, P. A., McClelland, J. W., Holmes, R. M., Zhulidov, A. V., Mull, K., Peterson, B. J.,
488 Striegl, R. G., Aiken, G. R., and Gurtovaya, T. Y.: Flux and age of dissolved organic carbon
489 exported to the Arctic Ocean: A carbon isotopic study of the five largest arctic rivers, Global
490 Biogeochem. Cycles, 21, GB4011, doi:10.1029/2007GB002934, 2007.

491 Osburn, C. L., Retamal, L., and Vincent, W. F.: Photoreactivity of chromophoric dissolved organic
492 matter transported by the Mackenzie River to the Beaufort Sea, Mar. Chem., 115,
493 doi:10.1016/j.marchem.2009.05.003, 2009.

494 Para, J., Charrière, B., Matsuoka, A., Miller, W. L., Rontani, J. F., and Sempéré, R.: UV/PAR
495 radiation and DOM properties in surface coastal waters of the Canadian shelf of the Beaufort
496 Sea during summer 2009, Biogeosciences, 10, 2761-2774, doi:10.5194/bg-10-2761-2013, 2013.

497 Ping, C.-L., Michaelson, G. J., Guo, L., Torre Jorgenson, M., Kanevskiy, M., Shur, Y., Dou, F., and
498 Liang, J.: Soil carbon and material fluxes across the eroding Alaska Beaufort Sea coastline, J.
499 Geophys. Res., 116, G02004, doi:10.1029/2010JG001588, 2011.

500 Rachold, V., Eiken, H., Gordeev, V. V., Grigoriev, M. N., Hubberten, H.-W., Lisitzin, A. P.,
501 Shevchenko, V. P., and Schirmeister, L.: Modern terrigenous organic carbon input to the Arctic
502 Ocean, in The Organic Carbon Cycle in the Arctic Ocean, edited by R. S. Stein and R. W.
503 Macdonald, 33–55, Springer, New York, 2004.

504 Rawlins, M. A., Steele, M., Holland, M., Adam, J., Cherry, J., Francis, J., Groisman, P., Hinzman, L.,
505 Huntington, T., Kane, D., Kimball, J., Kwok, R., Lammers, R., Lee, C., Lettenmaier, D.,
506 McDonald, K., Podest, E., Pundsack, J., Rudels, B., Serreze, M., Shiklomanov, A., Skagseth, O.,
507 Troy, T., Vorosmarty, C., Wensnahan, M., Wood, E., Woodgate, R., Yang, D., Zhang, K., and

© Author(s) 2017. CC BY 4.0 License.

Zhang, T.: Analysis of the Arctic System for Freshwater Cycle Intensification: Observations and Expectations, J. Climate, 23, 5715–5737, doi:10.1175/2010JCLI3421.1, 2010.

Raymond, P. A., McClelland, J. W., Holmes, R. M., Zhulidov, A. V., Mull, K., Peterson, B. J., Striegl, R. G., Aiken, G. R., and Gurtovaya, T. Y.: Flux and age of dissolved organic carbon exported to the Arctic Ocean: A carbon isotopic study of the five largest arctic rivers, Global Biogeochem. Cycles, 21, GB4011, doi:10.1029/2007GB002934, 2007.

Romanovsky, V. E., Drozdov, D. S., Oberman , N. G., Malkova, G. V., Kholodov, A. L., Marchenko, S. S., Moskalenko, N. G., Sergeev, D. O., Ukraintseva, N. G., Abramov, A. A., Gilichinsky, D. A., and Vasiliev, A. A.: Thermal State of Permafrost in Russia, Permafrost and Periglacial Process., 21, 136–155. doi:10.1002/ppp.683, 2010.

Semiletov, I., Pipko, I., Gustafsson, Ö., Anderson, L. G., Sergienko, V., Pugach, S., Dudarev, O., Charkin, A., Gukov, A., Bröder, L., Andersson, A., Spivak, E., and Shakhova, N.: Acidification of East Siberian Arctic Shelf waters through addition of freshwater and terrestrial carbon, Nature Geosci., 9, 361–365, doi:10.1038/ngeo2695, 2016.

Serreze, M., Barret, A. P., Slater, A. G., Woodgate, R. A., Aagard, K., Lammers, R. B., Steele, M., Mortitz, R., Meredith, M., and Lee, C. M.: The large-scale fresh water cycle of the Arctic, J. Geophys. Res., 111, C11010, doi:10.1029/2005JC003424, 2006.

Shiklomanov, I., Shiklomanov, A., Lammers, R., Peterson, B., and Vorosmarty, C.: The dynamics of river water inflow to the Arctic Ocean, in The Freshwater Budget of the Arctic Ocean, edited by E. Lewis, 281–296, Kluwer Acad., Boston, Mass, 2000.

Simon, E., Samuelsen, A., Bertino, L., and Mouysset, S.: Experiences in multiyear combined state-parameter estimation with an ecosystem model of the North Atlantic and Arctic Oceans using the Ensemble Kalman Filter, J. Mar. Syst., 152, 1–17, doi:10.1016/j.jmarsys.2015.07.004.

Stein, R., and Macdonald, R. W.: The Organic Carbon Cycle in the Arctic Ocean, Springer, Heidelberg, Germany, 2015.

© Author(s) 2017. CC BY 4.0 License.

Stow, A. C., Jolliff, J., McGillicuddy Jr., D. J., Doney, S. C., Allen, J. I., Friedrichs, M. A. M., Rose, K. A., and Wallhead, P.: Skill Assessment for coupled biological/physical models of marine systems, J. Mar. Syst., 76, 4–15, doi:10.1016/j.jmarsys.2008.03.011, 2009.

Tank, S. E., Manizza, M., Holmes, R. M., McClelland, J. W., and Peterson, B. J.: The Processing and Impact of Dissolved Riverine Nitrogen in the Arctic Ocean, Estuar. Coasts, 35, doi:10.1007/s12237-011-9417-3, 2012.

Tank, S. E., Striegl, R. G., McClelland, J. W., and Kokelj, S. V: Multi-decadal increases in dissolved organic carbon and alkalinity flux from the Mackenzie drainage basin to the Arctic Ocean, Environ. Res. Lett., 11, 054015, doi:10.1088/1748-9326/11/5/054015, 2016.

Tanski, G., Couture, N., Lantuit, H., Eulenburg, A., and Fritz, M.: Eroding permafrost coasts release low amount of dissolved organic carbon from ground ice into the nearshore zone of the Arctic Ocean, Global Biogeochem. Cycles, 30, 1054–1068, doi:10.1002/2015GB005337, 2016.

Tarnocai, C., Canadell, J. G., Schuur, E. A. G., Kuhry, P., Mazhitova, G., and Zimov, S.: Soil organic carbon pools in the northern circumpolar permafrost region, Global Biogeochem. Cycles, 23, GB2023, doi:10.1029/2008gb003327, 2009.

Taylor, K. E.: Summarizing multiple aspects of model performance in a single diagram, J. Geophys. Res.,106, 7183–7192, 2001.

Timmermans, M.-L.: Sea Surface Temperature, Arctic Report Card: Update for 2016, http://www.arctic.noaa.gov/Report-Card/Report-Card-2016/ArtMID/5022/ArticleID/285/Sea-Surface-Temperature, 2016.

Vallières, C., Retamal, L., Osburn, C., and Vincent, W. F.: Bacterial production and microbial food web structure in a large Arctic river and the coastal Arctic Ocean, J. Mar. Syst., 74, 756–773, doi:10.1016/j.jmarsys.2007.12.002, 2008.

Vaquer-Sunyer, R., Duarte, C. M., Santiago, E., Wassmann, P., and Reigstad, M.: Experimental evaluation of planktonic respiration response to warming in the European Arctic sector, Polar

© Author(s) 2017. CC BY 4.0 License.

558 Biol., 33, 1661–1671, doi:10.1007/s00300-010-0788-x, 2010.

559 Yang, D., Shi, X., and Marsh, P.: Variability and extreme of Mackenzie River daily discharge during

560 1973-2011, Quatern. Internat., 380–381, 159–168, doi:10.1016/j.quaint.2014.09.023, 2015.